Electronic Supplementary Material (ESI) for Journal of Materials Chemistry A.
This journal is © The Royal Society of Chemistry 2015

Supporting Information

Doping-Induced Structural Evolution from Rutile to Anatase: Formation of Nb-Doped Anatase TiO_2 Nanosheets with High Photocatalytic Activity

Hsin-Yi Wang,[§a] Jiazang Chen,[§a] Fang-Xing Xiao,[a] Jianwei Zheng,[b] and Bin Liu*[a]

[a]School of Chemical and Biomedical Engineering, Nanyang Technological University, 62 Nanyang Drive, Singapore 637459, Singapore

[b]Institute of High Performance Computing, Agency for Science, Technology and Research, 1 Fusionopolis Way, #16-16 Connexis, Singapore 138632, Singapore

§ These authors contributed equally to this work.

Email: liubin@ntu.edu.sg

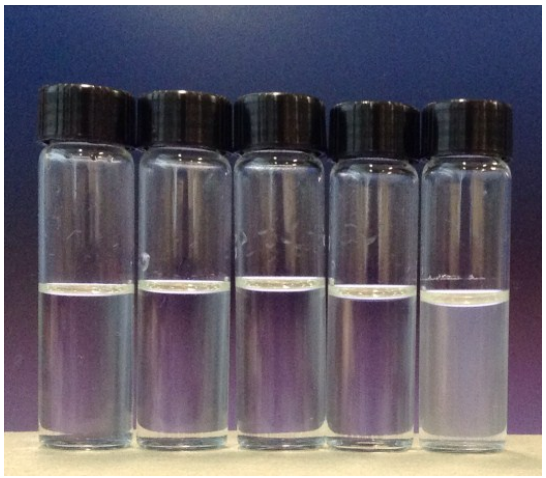

Figure SI-1. Stability characteristics of the hydroxo-aquo ions of titanium precursors in high acidic solution (6 M HCl). The five bottles from left to right contain the solutions hydrothermally treated at room temperature, 50 ºC, 80 ºC, 100 ºC, and 120 ºC for 6 hours, respectively. In this photograph, it is clear to see that titanium precursors are stable in acidic solution at low temperature (< 100 ^{o}C); while they become unstable once temperature increases (> 100 ^{o}C).

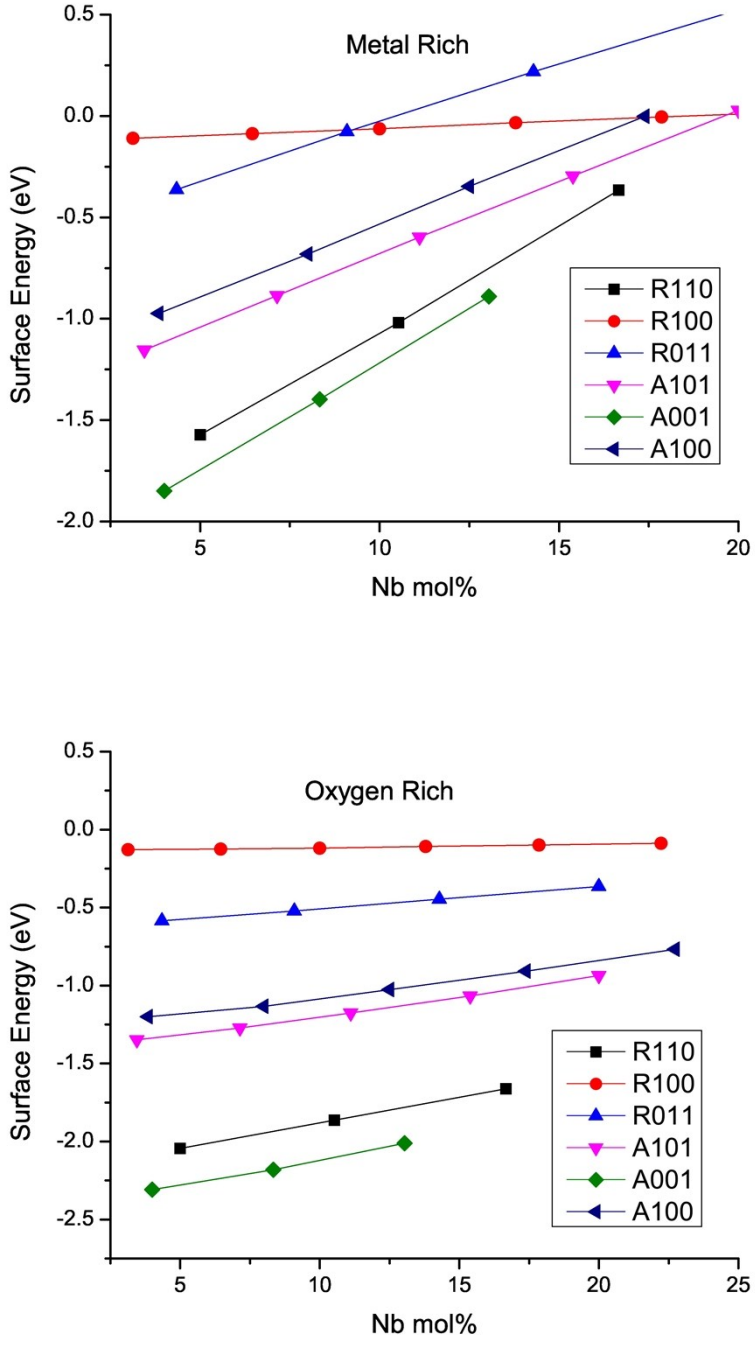

Figure SI-2. Surface free energy simulation on different TiO_2 facets.

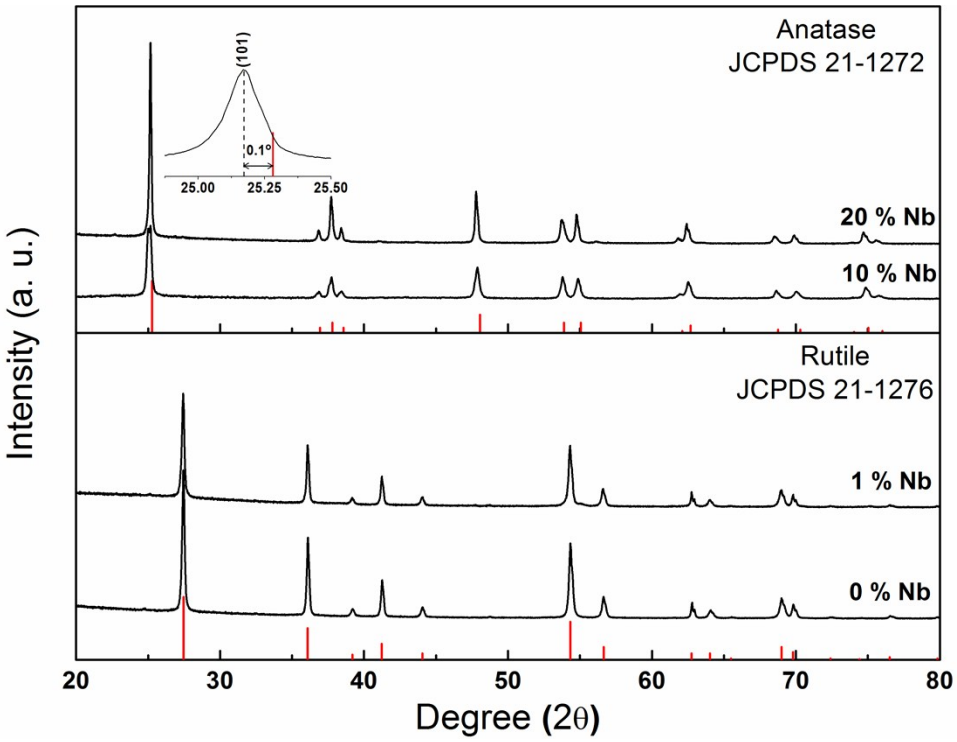

Figure SI-3. Crystalline information of Nb-doped TiO_2. XRD patterns of TiO_2 nanostructures doped with 0 % Nb, 1 % Nb, 10 % Nb, and 20 % Nb. From which, it is clear to see the phase of TiO_2 crystals evolve from rutile to anatase.

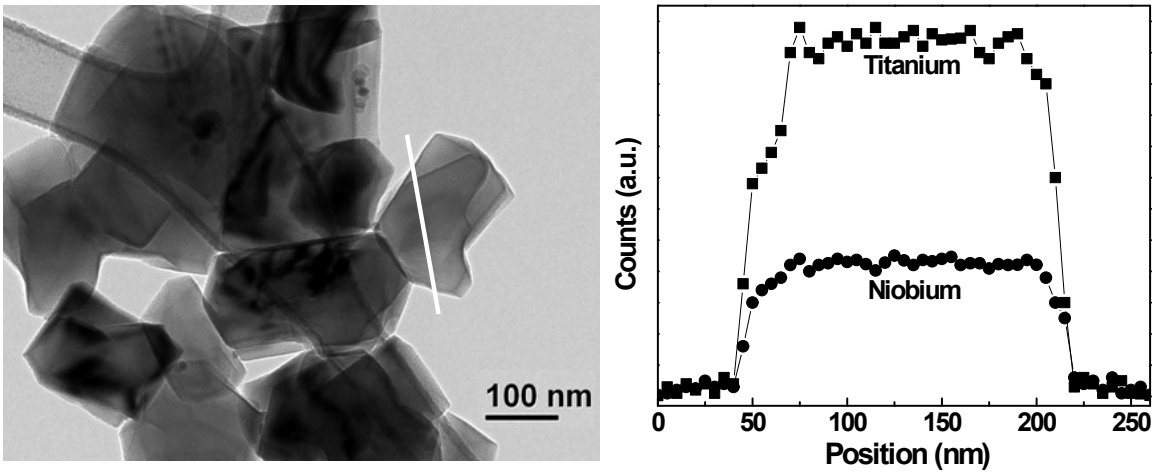

Figure SI-4. Elemental distribution of anatase Nb (10 %)-TiO_2. TEM image of anatase Nb (10 %)-TiO_2 multifaceted nanoparticles and the corresponding energy dispersive spectroscopy element line-scan profiles across an individual nanoparticle.

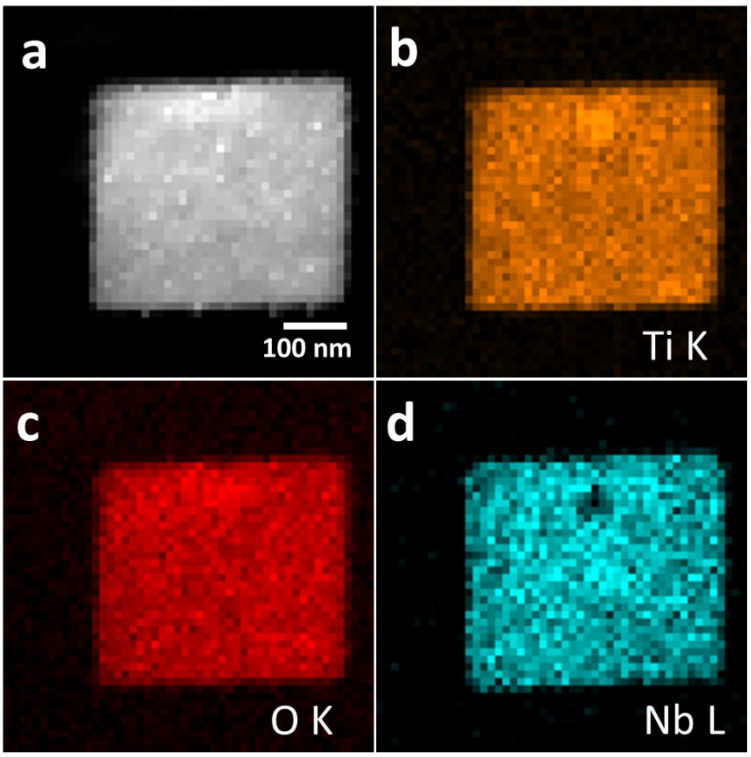

Figure SI-5. Elemental distribution of Nb (20 %) TiO_2. a) STEM image of a single anatase Nb (20 %)-TiO_2 nanosheet. EELS mapping images of b) titanium, c) oxygen, and d) niobium elements.

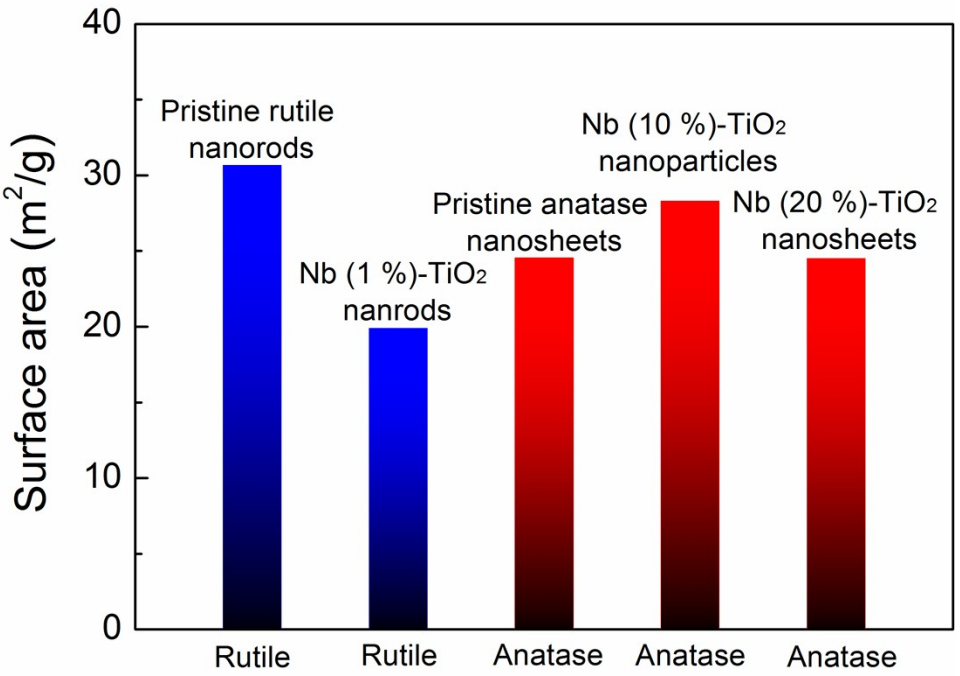

Figure SI-6. Specific surface area of pristine rutile nanorods, Nb (1 %)-TiO_2 nanorods, pristine anatase nanosheets, Nb (10 %)-TiO_2 nanoparticles, and Nb (20 %)-TiO_2 nanosheets.

Note: After doping 1 % Nb, the Nb (1 %)-TiO_2 nanorods become shorter and thicker as compared to the pristine rutile nanorods. Therefore, the specific surface area decreases a little bit. However, after introducing 10 % and 20 % Nb, the specific surface area of Nb (10 %)-TiO_2 nanoparticles and Nb (20 %)-TiO_2 nanosheets keep nearly the same as the pristine rutile nanorods. Additionally, the specific surface area of pristine anatase nanosheets is almost identical to that of Nb (20 %)-TiO_2 nanosheets. Therefore, the effect of change in surface area on the photocatalytic activity should be marginal.

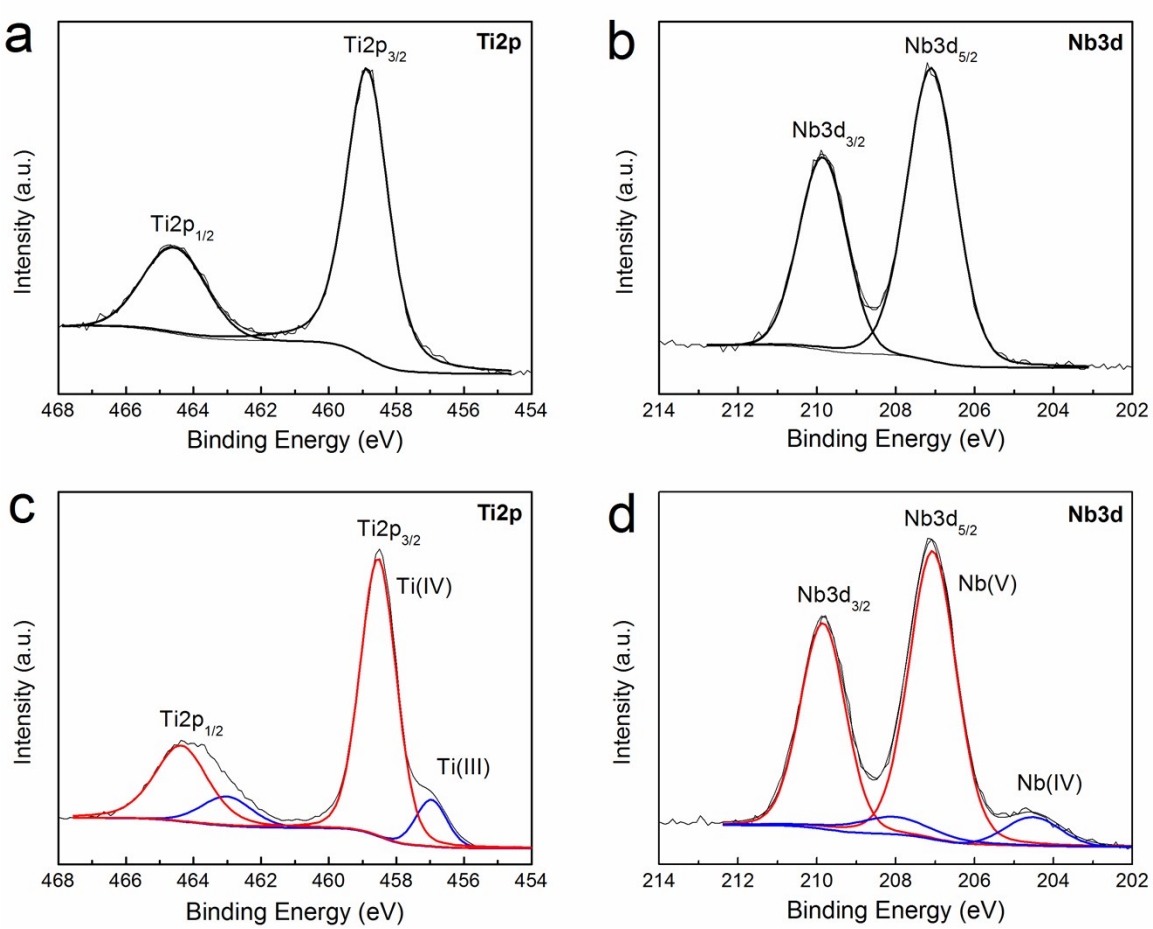

Figure SI-7. Elemental chemical states of Nb (20 %)-TiO_2 nanosheets. a,b) High-resolution XPS spectra of Ti2p and Nb3d. c,d) High-resolution XPS spectra of Ti2p and Nb3d after Ar^+ polishing for 30 min. The additional Ti^{3+} and Nb^{4+} signals could be detected as the result of charge compensation.

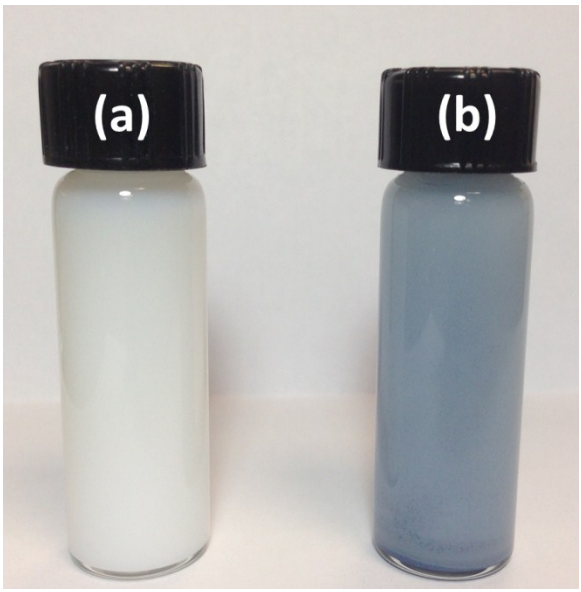

Figure SI-8. Digital photographs of a) pristine rutile TiO_2 nanorods and b) anatase Nb (20 %)-TiO_2 nanosheets suspension.

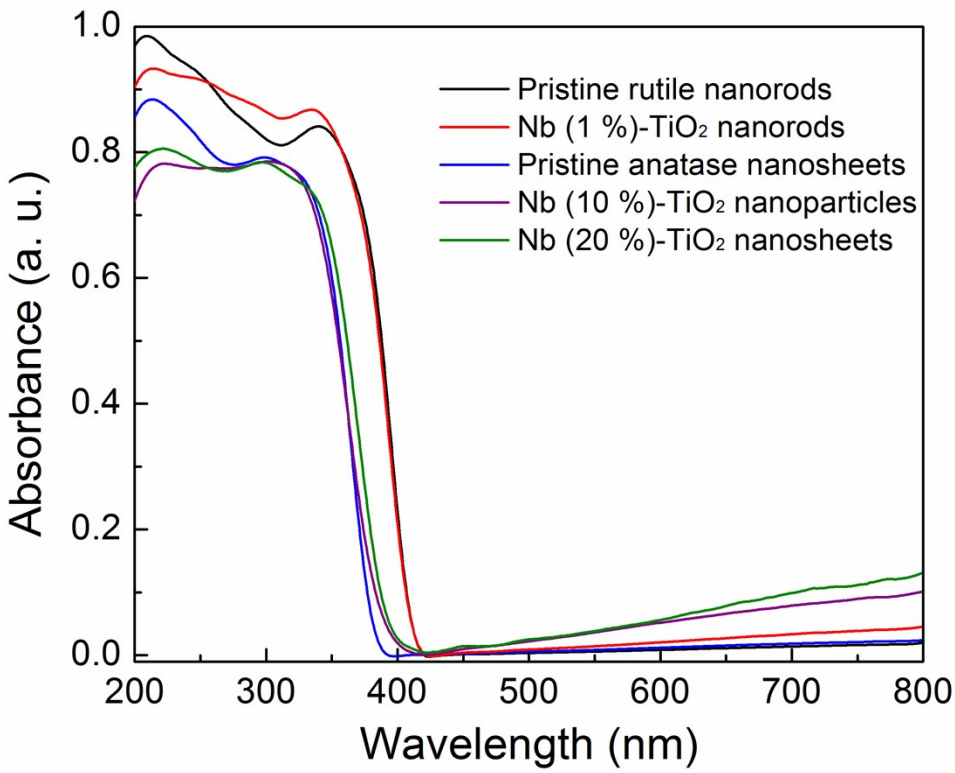

Figure SI-9. UV-vis diffuse reflectance spectra (DRS) of different TiO_2 samples.

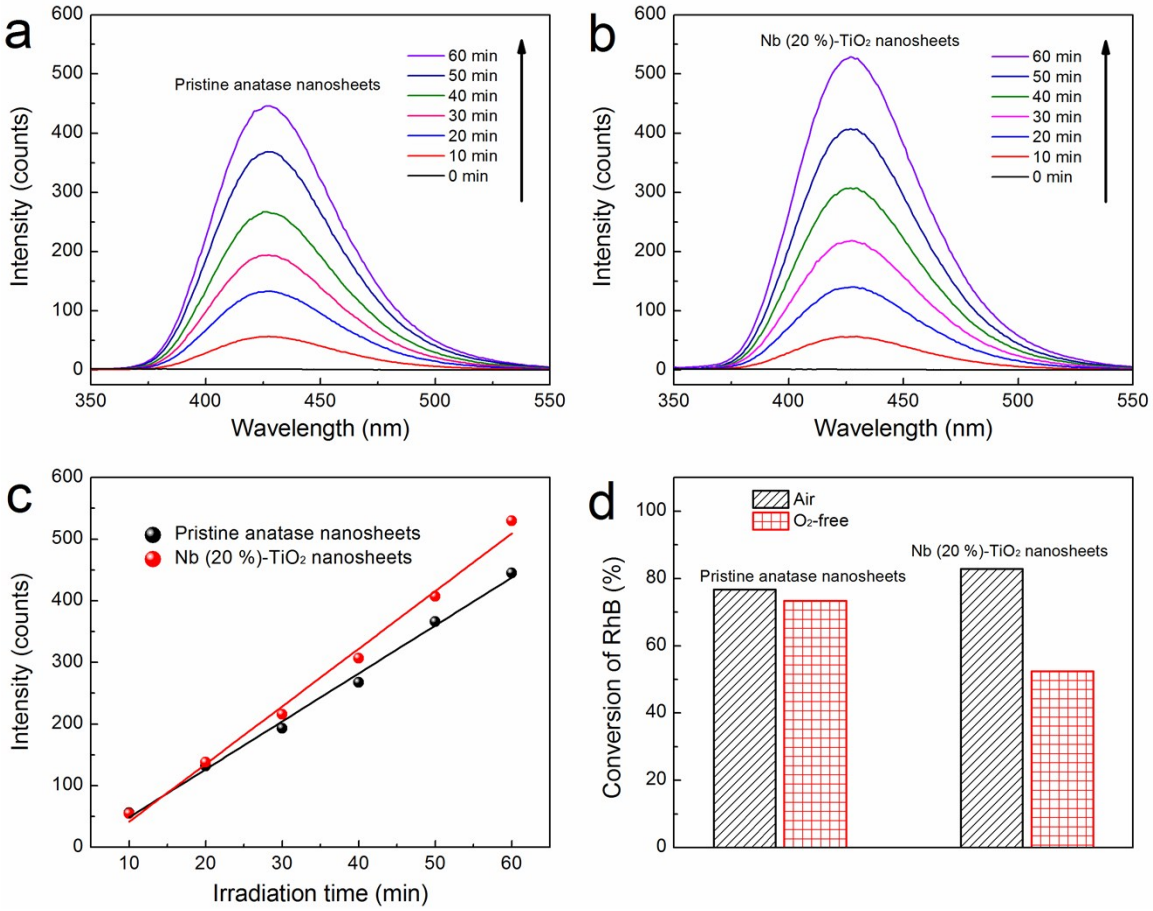

Figure SI-10. ·OH-trapping PL spectra of (a) pristine anatase nanosheets and b) anatase Nb (20 %)-TiO_2 nanosheets in an aqueous solution under UV light irradiation. c) Fluorescence intensity of luminol as a function of irradiation time for pristine anatase nanosheets and anatase Nb (20 %)-TiO_2 nanosheets. d) Comparison of photocatalytic performances between pristine anatase nanosheets and anatase Nb (20 %)-TiO_2 nanosheets at ambient conditions and in an anoxic environment (O_2-free, argon saturated condition) under UV light illumination for 60 min.

Adsorption of O_2 on pristine and Nb-doped TiO_2 surface

The adsorption of O_2 on rutile (011) and anatase (001) surfaces was calculated using density functional theory, which is implemented in *Vienna ab initio Simulation Package* (VASP) program. The electron-ion interaction is modeled by the projector-augmented wave (PAW) method. The Perdew-Burke-Ernzerhof form of generalized gradient approximation (GGA) was used for the exchange and correlation functional. The plane-wave cutoff energy was set to 520 eV. The Monkhost-Pack *k*-point sampling was tested to be 3 × 3 × 1. We have tested various adsorption positions and found they converged to bridge (Ti/Nb at the middle of O-O bond) after relaxation. **Table SI-1** lists the adsorption energies. Obviously, O_2 prefers to adsorb on Nb site.

Table SI-1. Adsorption energies of O_2 on anatase (001) and rutile (011) surfaces

	Anatase (001)		Rutile (011)	
	Nb	Ti	Nb	Ti
E_{adsorb} (eV)	-1.88	-0.63	-3.87	-0.47